

Influence of cyclic fatigue on the mechanical properties of amorphous polycarbonate

Xiaowei Li*, Hristo A. Hristov and Albert F. Yee†

Department of Materials Science and Engineering, University of Michigan, Ann Arbor, Michigan 48109, USA

and David W. Gidley

Department of Physics, University of Michigan, Ann Arbor, Michigan 48109, USA
(Received 26 August 1994)

Changes in the mechanical properties of amorphous polycarbonate during the fatigue failure initiation stage lead to overall embrittlement of the polymer. The results indicate that the fracture toughness of the material can be reduced by ~35% without visible damage. The 'static' mechanical characteristics, such as yield stress and strain and absorbed energy, are influenced very modestly by the cyclic fatigue. The observations are explained by the presence of a small number of nanometre-sized voids or 'protocrazes', detected by transmission and scanning electron microscopy measurements. It is shown that physical ageing and fatigue loading affect the structural state of the polymer differently despite similar effects on the macroscopic mechanical properties.

(Keywords: cyclic fatigue; polycarbonate; mechanical properties)

INTRODUCTION

Plastic parts have been used increasingly as structural elements in instruments and devices that are subjected to long-term stress fluctuations. Such use has prompted an increased interest in their mechanical performance when subjected to low-level load variations commonly known as fatigue. It has long been recognized^{1,2} that it is desirable to be able to influence or at least predict the fatigue failure of the commonly used engineering thermoplastics.

The fatigue failure of thermoplastics generally develops in two phases^{1–3}. First, the material accumulates fatigue damage (i.e. in the initiation phase), which ultimately leads to the formation of visible crazes. The crazes further grow, form cracks and propagate (i.e. in the propagation phase) until final failure occurs. The amount of material published on this subject is quite extensive and there are several excellent monographs and review articles summarizing progress in this area^{1,3–6}. Most of the investigations are dedicated to the determination of fatigue lifetime as a function of external variables such as stress amplitude (*S–N* curves), temperature, test frequency, environment and others^{1,3,4}. It has been established that the fatigue lifetime of most polymers is very sensitive to external fields, and as a rule is much shorter than the

corresponding lifetime under constant stress. The role of material parameters, such as molecular weight and weight distribution, branching, crosslink density, blending and inclusions, among others, has also been a subject of considerable interest^{1,3,6}. Results from these references indicate that the combined effect of the 'internal' and 'external' variables can be rather complex. However, most of the phenomena characterizing the propagation phase can be interpreted as competition between the propensity of the material to undergo shear deformation or to develop crazes^{5,7}.

A significant amount of experimental work has also been performed on precracked specimens, by measuring the extent of crack growth as a function of variation in the stress concentration (ΔK) at the crack tip^{1,7–9}. It has been found that the crack propagation of most plastics, beyond the threshold region, can be described by a simple power law—the well known Paris equation.

The structural investigations have been devoted mainly to the dynamics of craze/crack propagation by using optical interference methods⁸. *In situ* small-angle X-ray scattering (SAXS) measurements of amorphous polystyrene in cyclic bending at high stress amplitudes¹⁰ demonstrate that buckling and coalescence of craze fibrils are the most important mechanisms in the fatigue craze breakdown in thermoplastics. The structural features commonly present on fatigue fracture surfaces^{6–8} have been investigated by using optical microscopy and scanning electron microscopy (SEM).

*Present address: Michigan State University, Department of Materials Science and Engineering, East Lansing, MI 48823, USA

†To whom correspondence should be addressed

The changes in the materials properties during fatigue loading have been examined by measuring *in situ* the stress-strain hysteresis curves, temperature, cyclic modulus, dynamic modulus (E'), $\tan \delta$, etc.^{1,4,11,12} The results of these studies demonstrate that, when the stress amplitude ($\Delta\sigma$) is high and/or the test frequency is high, heat generated in the sample leads to a widening of the hysteresis loops and an increase of the sample temperature, resulting in fatigue softening of the polymer and rapid fracture. At low to moderate stress amplitudes, test frequency (i.e. moderate heat generation), the material properties appear to be fairly stable until the final stage of the fatigue, when the specimen fails rapidly.¹

Despite this relatively extensive information, very few works have been dedicated to the initiation phase of the fatigue process. On several occasions the number of cycles required for initiation of structural inhomogeneities in the material has been reported^{1,3}. The results of these works show that the initiation time can be a major fraction of the total fatigue lifetime, especially at low stress amplitudes. It is also known that fatigue loading generally embrittles the polymers, but the experimental information is very sparse and it is still not clear what kind of structural changes cause the deterioration of the performance of the polymers. Since physical ageing (i.e. annealing below the glass transition temperature) also embrittles polymeric materials, the role of mechanical loading on the ageing kinetics in amorphous polymers has been discussed extensively^{13–15}. Despite some claims, direct structural correlation between the two processes has not been established, and it is not clear whether such correlation exists at low load amplitudes.

Fatigue failure initiation in semicrystalline polyoxymethylene (POM) has been investigated by SAXS, and the results are interpreted as formation of small voids at the crystalline-amorphous interphase boundary¹⁶. Our group recently reported SAXS and transmission electron microscopy (TEM) studies^{17,18} of fatigue craze initiation in amorphous polycarbonate. We demonstrated in these studies that the accumulation of fatigue damage leads to formation of one or more nanometre-sized voids, which later grow into visible crazes.

The goal of the present work is to investigate the fatigue-induced changes in the mechanical properties of amorphous polycarbonate, with a focus on the initiation phase. An attempt is made to correlate results from macroscopic mechanical measurements with the microscopic results obtained via TEM and SEM methods.

EXPERIMENTAL

Material

The material used in this research is amorphous polycarbonate (PC) produced by the Dow Chemical Company, with molecular weight $M_w = 37\,200$, as determined by gel permeation chromatography (g.p.c.) calibrated by light scattering. The PC pellets were dried for 12 h in vacuum at 100°C and compression moulded into 1/4 inch (~6.3 mm) thick sheets. Smooth dumbbell-shaped specimens with gauge length of 30 mm and width of 12.7 mm (1/2 inch) were machined from the sheets. After another vacuum drying, the samples were annealed at 160°C ($T_g \sim 150^\circ\text{C}$) for 45 min to erase the residual stresses from the cutting procedure. Finally the samples

were cooled rapidly (200 °C min⁻¹) to room temperature, and the so-prepared 'fresh' specimens with identical stress and thermal history were used for further ageing and/or fatigue experiments. The samples were aged in the temperature interval 60–130 °C, for time periods up to 1500 h.

Fatigue

The specimens were fatigued using a computer-controlled servohydraulic testing machine (Instron 1331) in the load control mode, with loads corresponding to maximum stresses in the range 10–40 MPa (yield stress $\sigma_y = 61$ MPa at a strain rate of 0.0787 min⁻¹ at 25 °C) at a constant temperature of 55 °C. The fatigue was performed in the tension regime ($\sigma_{\min} = 0$), with a sinusoidal waveform, and a test frequency of 5 Hz. Since we are mainly interested in fatigue failure initiation, the fatigue test was usually interrupted before development of visible crazes. *In situ* measurements of the sample temperature were performed by using a thermocouple glued to the surface of the specimens. The respective volume changes, as a function of the number of cycles at some particular stress amplitude, were recorded by a pair of surface strain gauges mounted perpendicularly to each other, one parallel and the other perpendicular to the fatigue stress. Owing to the viscoelastic nature of the polymers, the sample volume does not decrease to its initial value when the stress decreases to zero at the end of each cycle. From the readings of the strain gauges at the moment when the stress is zero, one can determine the cyclic residual volume as a function of the number of cycles at some particular stress amplitude by using:

$$(\delta V_i/V)_{\sigma=0} = (1 + \epsilon_{il})(1 + \epsilon_{ip})^2 - 1 \quad (1)$$

where ϵ_{il} and ϵ_{ip} are the residual strains parallel and perpendicular to the stress direction, respectively, at stress zero during the i th cycle. From the readings of the strain gauges during each cycle, one can also derive the running cyclic modulus:

$$E_i = \sigma_{\max}/(\epsilon_{i,\max} - \epsilon_{i,\min}) \quad (2)$$

where $\epsilon_{i,\max}$ and $\epsilon_{i,\min}$ are the maximum and minimum values of the longitudinal strain for the i th cycle, and σ_{\max} is the stress amplitude. Thus, E_i corresponds to the secant modulus in monotonic loading.

Mechanical testing

The mechanical properties of both the fatigued specimens and the physically aged samples were further investigated by using a screw-driven testing machine (Instron 4502). The tensile tests were performed by loading the specimens to their yield point and subsequently unloading them to zero stress at a strain rate of 0.0787 min⁻¹. In Figure 1 is shown the stress-strain curve of a fresh PC sample, and with reference to this figure the parameters that can be derived from the loading/unloading experiments are as follows: σ_A , yield stress; ϵ_D , yield strain; ϵ_B , residual strain immediately after reducing the stress to zero; ϵ_C , final residual strain after 12 h relaxation at room temperature; U_t , the total energy of deformation, which is the area under the curve OA; U_e , the elastic energy of deformation, which is the area under the curve BA; and U_p , the plastic component of the total energy ($U_t - U_e$).

The fracture toughness of the various specimens was

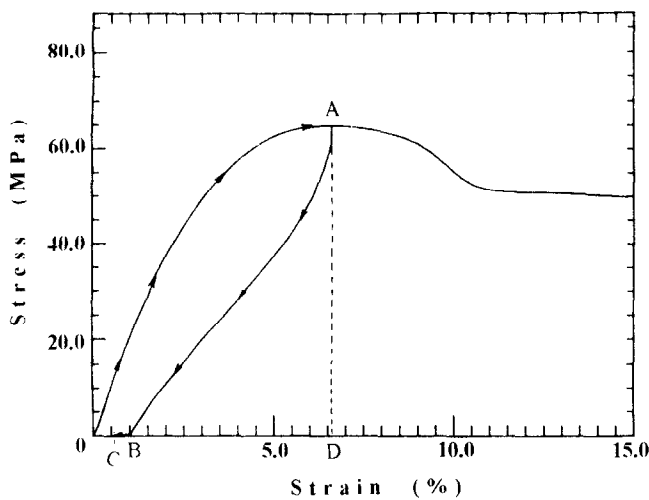


Figure 1 Stress-strain curve of 'fresh' polycarbonate

derived according to the *J*-integral *R*-curve method^{19,20}, by using series of identically precracked samples. After loading to various displacements, the unloaded samples were broken open in liquid nitrogen and photographs of the crack extensions were analysed by computer.

Scanning and transmission electron microscopy

Some of the fatigued specimens and a number of non-fatigued control samples were frozen in liquid nitrogen and broken along a plane perpendicular to the original fatigue stress direction. The fracture surfaces were coated with $\sim 200 \text{ \AA}$ gold-palladium film, and examined on a Hitachi-S800 SEM at an accelerating voltage of 2 kV. All of the fatigued samples used for SEM studies were free of visible crazes, as determined by optical microscopy (at $60\times$).

The TEM investigations were performed on thin slices (50–300 nm) microtomed from the fatigued specimens by using a Reichert-Jung ultramicrotome at room temperature. The microtoming was executed in such a manner that the original stress direction is always in the plane of the thin slices. The microtomed slices were examined without further preparation on a JEOL 4000 electron microscope at acceleration voltage of 400 kV. (More experimental details on the microtoming procedures and the TEM measurements are reported in ref. 18.)

RESULTS

In situ measurements

In Figure 2 is shown the change of the surface temperature of fresh samples as functions of the stress amplitude and number of cycles. It is clear that the heat generation is not excessive and after 1500–2000 cycles the temperature equilibrates. It can be computed (from the sample thickness, thermal conductivity and density of PC) that at a stress amplitude of 30 MPa the temperature in the central part of the specimen is $\sim 1^\circ\text{C}$ higher than the surface temperature. For lower stress amplitudes this difference is correspondingly smaller. The increase of the temperature leads to initial decrease of the fatigue modulus (Figure 3), computed by using equation (2), but after ~ 2000 cycles the strain softening

is negligible for all stress amplitudes at the test frequency used (5 Hz).

The cyclic residual volume, computed by using equation (1), increases rapidly at the beginning of the fatigue process (following the temperature trend), but subsequently levels off (Figure 4). It should be noted that the residual volume increase is due to several interrelated factors such as stress amplitude, temperature, non-zero average stress (creep component) and possibly the damage resulting from the cyclic loading. The increase of the stress amplitude increases the sample temperature, leading to thermal volume expansion. On the other hand, the increase in the temperature causes a decrease in the modulus, thus changing the viscoelastic properties of the

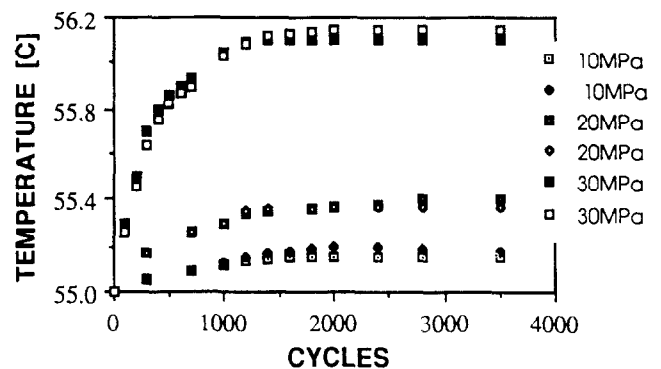


Figure 2 Surface temperature as a function of the number of cycles (stress amplitudes are indicated in the figure)

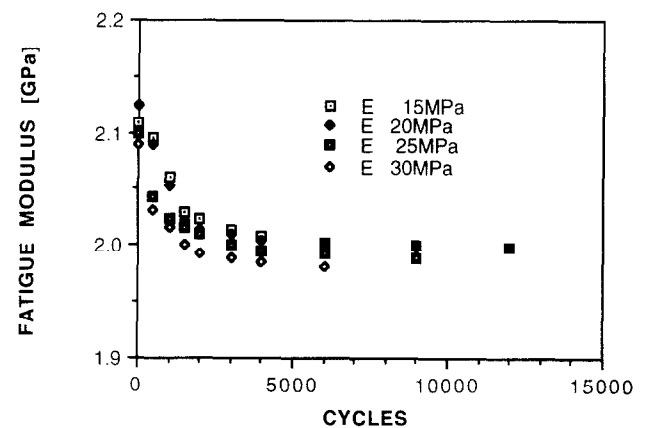


Figure 3 Fatigue modulus as a function of the number of cycles (stress amplitudes are indicated in the figure; see text for details)

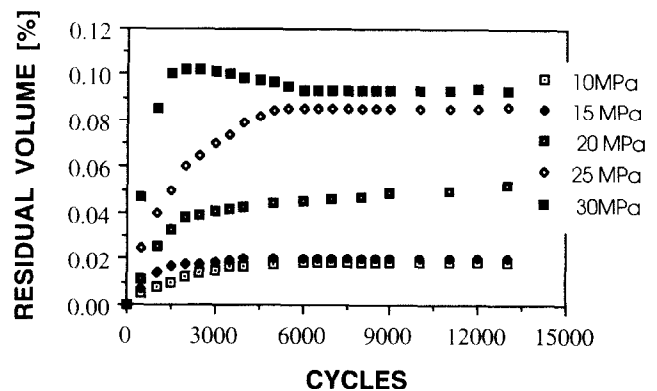


Figure 4 Residual volume as a function of the number of cycles (stress amplitudes are indicated in the figure; see text for details)

polymer, the resultant contribution from the creep component and the extent of the material's relaxation within each cycle. While it is difficult to distinguish among the various contributions, the individual factors generally increase the specific volume of the material. Residual strain measurements performed after the end of the fatigue loading demonstrated that the specific volume is higher than its initial value (before the fatigue), even after 12 h of relaxation at zero stress. Based on the analysis of the *in situ* data, we concluded that permanent structural changes (if any) in the specimens used in the present study do not result from intensive heat generation. The experiments were carried out at relatively low temperatures and for short times, which precludes any significant chemical reactions, thus any changes in the materials properties should be attributed to the accumulation of fatigue damage.

Loading-unloading experiments and fracture toughness results

The loading and unloading experiments performed after the fatigue was stopped showed systematic changes in the mechanical properties with increasing stress amplitude. These changes include a decrease of the total and residual energies (Figure 5), residual strain (not shown here) and yield strain (Figure 6), while the yield stress increases somewhat (Figure 7). The fresh samples used for this set of measurements were fatigued for 25 000 cycles under constant load control. Optical observations revealed that the specimens fatigued with stress amplitudes of 25 and 30 MPa contain visible crazes, and higher stress produced higher craze density. The rest of the specimens appeared visually homogeneous.

Samples subjected to various fatigue histories were compared with those subjected to various ageing histories. The results show similar trends when the change in the mechanical properties of the fatigued specimens as a function of the stress amplitude at constant number of

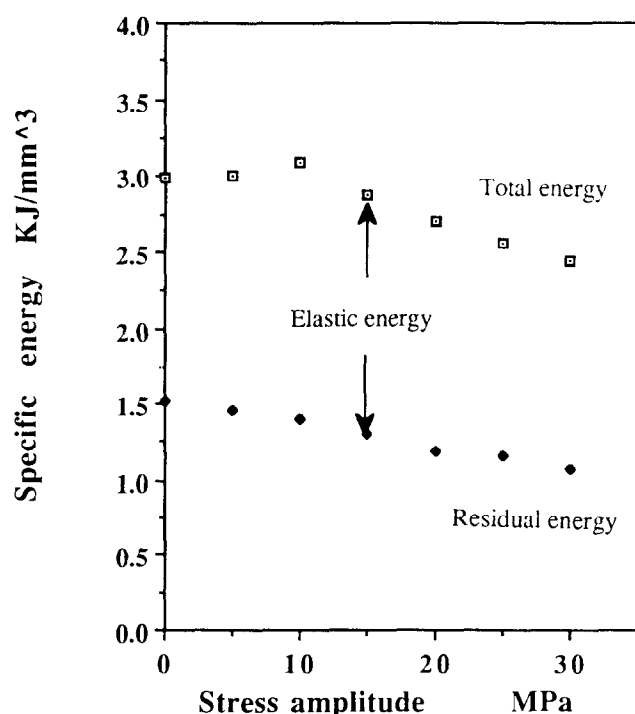


Figure 5 Change of the absorbed energies as a function of the stress amplitude (samples fatigued for 25 000 cycles at 5 Hz; see text for details)

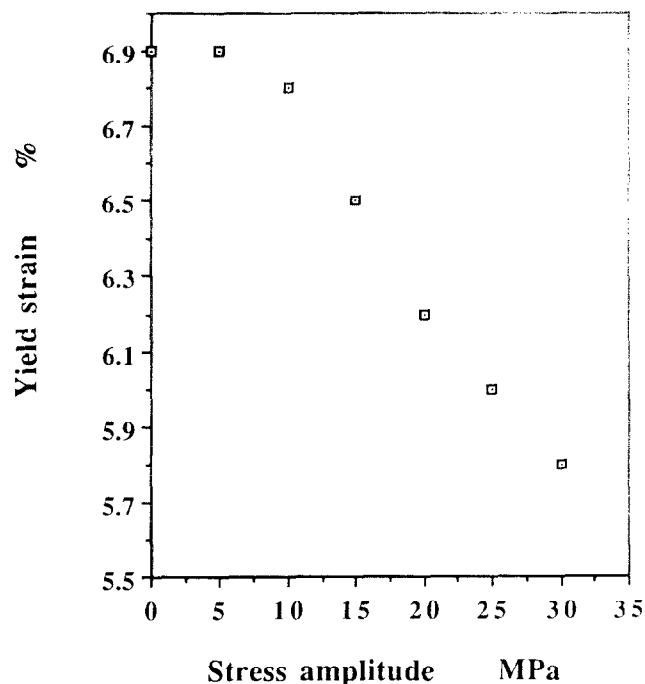


Figure 6 Yield strain as a function of the stress amplitude (samples fatigued as in Figure 5)

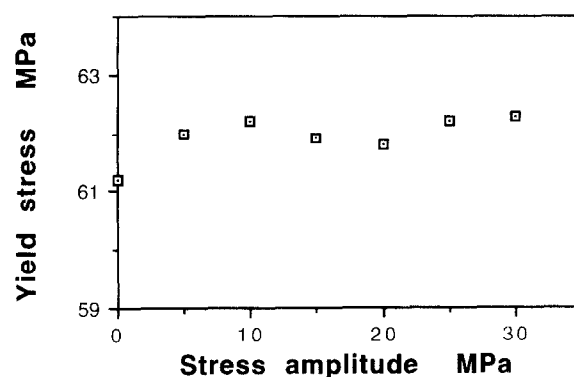


Figure 7 Yield stress as a function of the stress amplitude (samples fatigued as in Figure 5)

cycles is compared to the respective variation in samples aged at a constant temperature with increasing time periods (Figures 5–7 vs. Figures 8–10). The same result (not shown here) is observed if the material is aged at increasing temperatures (below T_g) for a fixed time period. The changes of the mechanical properties of the aged material, as expected, are influenced by both the ageing temperature and the ageing times.

The gradual change of the material performance described above, while measurable, is relatively small. It seems that fatigue loading has a negligible effect on the absorbed energy (Figure 5) and the yield stress (Figure 7). Our investigations revealed that cyclic fatigue and physical ageing affect more substantially the fracture toughness of the amorphous polycarbonate. In Figure 11 are summarized the measurements of the fracture toughness of the material as functions of the stress amplitude and ageing time (ageing temperature 100 °C). The specimens used for this set of measurements were fatigued for 10 000 cycles at the stress amplitudes indicated in the figure. Optical observations revealed that

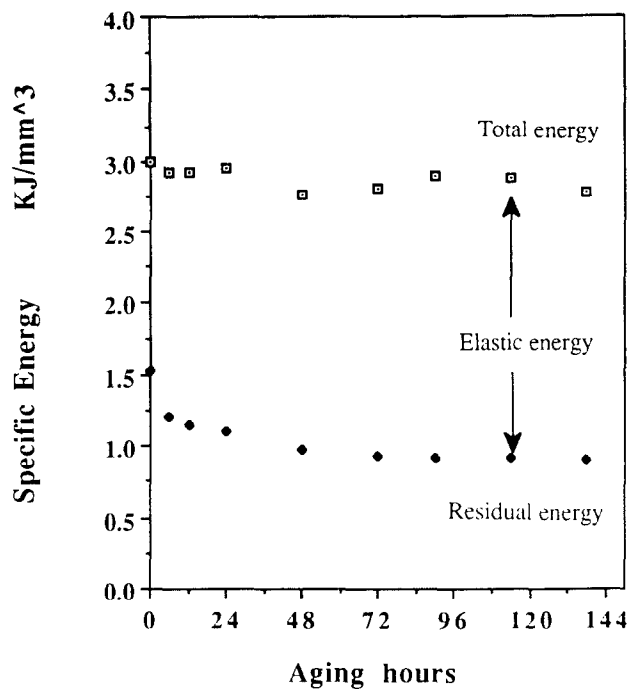


Figure 8 Change of the absorbed energies as a function of the ageing time (samples aged at 100 °C)

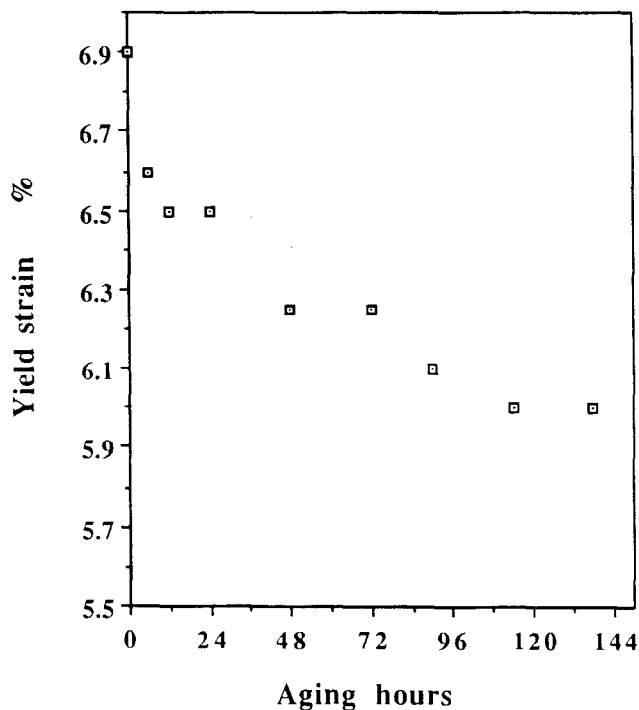


Figure 9 Yield strain as a function of the ageing time (samples aged at 100 °C)

all specimens were craze-free at the end of the fatigue loading. The multi-sample *R*-curve method requires 7–10 specimens for each particular stress amplitude, and since the measurements were repeated for 3–5 samples, each point in the figure is determined by testing 40–50 specimens. From the results in *Figure 11* it is seen that the combined effect of higher stress amplitudes and longer ageing times can reduce the fracture toughness by ~35% without any visible changes in the material.

Transmission and scanning electron microscopy

While optical microscopy did not show material discontinuities in the samples aged at 100 °C then fatigued for 10 000 cycles, the TEM investigation of microtomed slices from these specimens detected the presence of oblate voids with small dimensions parallel to the fatigue stress. In *Figure 12a* is shown a TEM micrograph of a

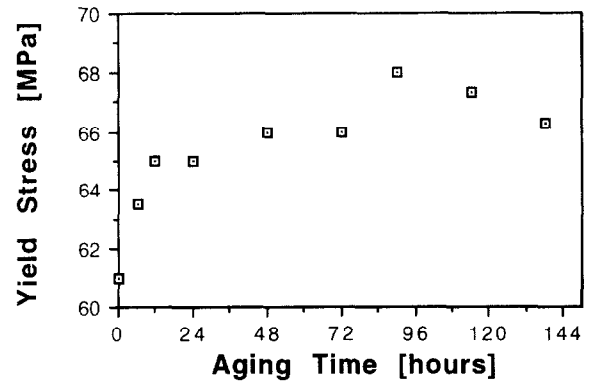


Figure 10 Yield stress as a function of the ageing time (samples aged at 100 °C)

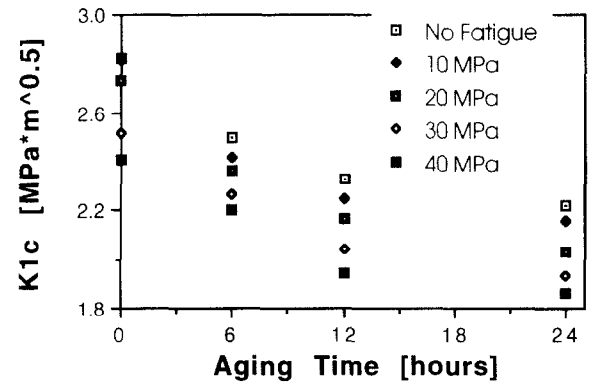


Figure 11 Fracture toughness dependence on the stress amplitude and ageing time (specimens aged at 100 °C then fatigued for 10 000 cycles at the stress amplitudes indicated in the figure)

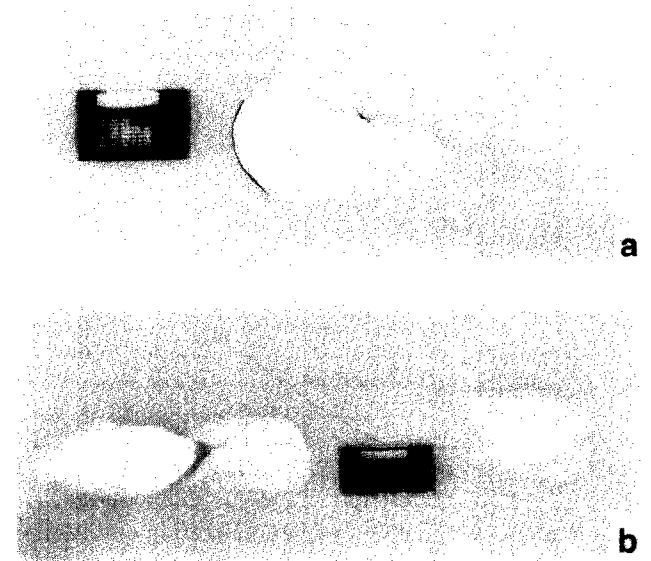


Figure 12 TEM micrographs of protocrazes in fatigued specimens: (a) initial void (protocraze); (b) advanced stage of fatigue protocraze development. Fatigue stress axis vertical

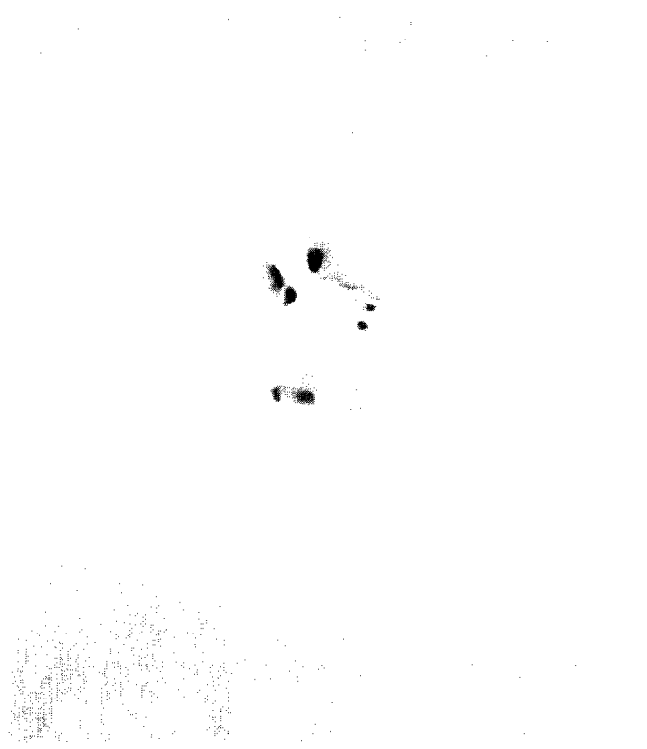


Figure 13 SEM micrograph of freeze-fracture surface of a specimen fatigued at 40 MPa for 10 000 cycles. Fatigue stress perpendicular to the fracture surface

fatigue-induced void with dimension ~ 100 nm in the direction parallel to the fatigue stress, and in *Figure 12b* a more advanced stage of the protocraze development. (For more details see ref. 18.)

In *Figure 13* is presented an SEM micrograph of the fracture surface of a fresh sample, fatigued at stress amplitude of 40 MPa for 10 000 cycles. Since fracture at room temperature is accompanied by plastic deformation, which may obscure the fracture surface structure, the samples used for SEM were broken at 77 K. The surface of the sample shown in *Figure 13* contains structural aggregations, which we interpret as a planar image of broken protocrazes (the fracture surface is perpendicular to the fatigue stress direction). No such formations were detected on the fracture surfaces of non-fatigued control specimens despite exhaustive searches. The fracture surfaces of the fatigued specimens outside the protocraze area appeared visually identical to the fracture surfaces of the control specimens.

DISCUSSION

The above-mentioned trends in the changes of the mechanical properties during fatigue failure initiation and physical ageing seem to imply that the structural changes underlying both processes should be similar too. It is well established that annealing at temperatures below the glass transition temperature reduces such excess thermodynamic quantities as entropy, enthalpy and volume^{21–23}. The reduction of the specific volume leads to a decrease of the molecular mobility, which ultimately embrittles the material as demonstrated in *Figures 8–11*. Thus, one possible explanation of the source of embrittlement in the amorphous polycarbonate upon fatigue loading is the reduction of the excess volume. The results

of the *in situ* measurements, however, show exactly the opposite – the cyclic residual volume increases with the increase of the stress amplitude (*Figure 4*). Even after 12 h of post-fatigue relaxation at zero stress, the samples fatigued for 10 000 cycles at $\sigma_{\max} = 20$ MPa exhibited a residual volume of $\sim 0.01\%$. Similarly the results from the relaxation experiments of specimens fatigued at different stress amplitudes showed that the macroscopic volume change is always positive. Further *in situ* microscopic measurements by using positron annihilation lifetime spectroscopy (p.a.l.s.) also indicate an increase of the ‘hole’ volume fraction, which is associated with higher excess volume, with increasing number of cycles and/or stress amplitudes²⁴. All of the above-discussed information suggests that the structural changes during physical ageing and fatigue failure initiation are completely different in nature.

Another possible reason for the fatigue-induced embrittlement of the amorphous PC is the eventual decrease of the molecular weight, i.e. extensive chain scission in the course of the cyclic loading. Taking into account that the stress amplitudes used in our experiments are generally $< \sigma_g/2$, along with the considerable mobility of the PC chains at the test temperature, the probability of chain scission must be considered very low. G.p.c. measurements on craze-free fatigued samples did not show any measurable change of the molecular weight and weight distribution. Differential scanning calorimetry measurements confirmed the absence of significant chain scission in the precraze stage since the T_g was constant regardless of the stress amplitude and/or number of cycles (a significant decrease in the molecular weight must be accompanied by a decrease in T_g). The increase of the specific volume of the fatigued samples is also inconsistent with significant decrease of the molecular weight, because shorter chains pack more efficiently, which reduces the specific volume. Our conclusion is that, while some very limited chain scission is not excluded prior to craze development in fatigued PC, its influence on the mechanical properties should be of minimal importance.

In the above discussion, we analysed possible contributions to the mechanical properties from global structural changes, i.e. structural changes affecting the entire active volume of the specimen. Recent investigations of fatigue failure initiation in PC by using SAXS and TEM^{17,18} demonstrate that the process is characterized by significant localization of the fatigue damage. In some random localities, the initiation starts with the formation of oblate voids or ‘protocrazes’ (see also *Figures 12a* and *12b*), while the rest of the material appears homogeneous. It is reasonable to assume that the presence of such ‘defects’, introduced by the fatigue, will affect the mechanical properties of the specimens. More specifically, if the protocrazes contribute to the reduced fracture toughness, one should be able to locate such formations on the freeze fracture surfaces of the fatigued specimens. As shown in *Figure 13*, one can detect an agglomeration of voids or ‘protocrazes’ with sizes in the nanometre range. The investigations also revealed that the number of protocraze formations similar to that shown in *Figure 13* increases with the increase of the stress amplitude: we found 3–5 ‘protocrazes’ per fracture surface at the highest amplitude (40 MPa) and less than one at the lowest one (10 MPa). Since the specimens are broken at arbitrary locations, it is difficult to quantify the volume number

density of voids, but it is clear that it is not very high even for the highest $\Delta\sigma$ used. To our understanding this low concentration of fatigue-induced defects, at the precraze stage, can explain the very modest changes of the 'static' mechanical properties, such as yield stress and strain and absorbed energies (Figures 5–7). On the other hand, the presence of even a small number of structural discontinuities can significantly alter the fracture resistance of the specimens. More detailed investigations are needed to elucidate further the effects of the microstructural damage on the mechanical properties of fatigued polymers, but it is clear that these effects can be substantial without any visible changes in the material.

Based on macroscopic measurements, some authors suggest that, despite the overall increase of the specific volume, the fatigue process induces non-uniform volume contraction during the precraze stage²⁵. Our measurements by SAXS¹⁷, TEM¹⁸ and SEM (present work) clearly demonstrate that there is no evidence of such volume contraction or localized densification. It is quite possible, however, that in some small volumes the fatigue changes the molecular parameters; for example, the cyclic loading may generate regions with reduced entanglement density. Such regions may further serve as initiation sites for fatigue-induced protocrazes.

CONCLUSIONS

The results reported in the present work demonstrate that the damage accumulated in the fatigue failure initiation phase has a limited effect on the 'static' mechanical properties of the amorphous polycarbonate. The effects on the fracture resistance (fracture toughness) of the polymer are much more significant. It is demonstrated that the fatigue embrittlement of the material is fundamentally different from the embrittlement caused by physical ageing, despite the similar trends in their mechanical properties. The fatigue-induced embrittlement, in the precraze stage, most probably results from generation of material discontinuities in the shape of oblate voids or 'protocrazes'.

ACKNOWLEDGEMENTS

This research is supported by the US Department of Energy, Grant No. DE-FGO2-88ER-45366. We thank the Dow Chemical Co. for supplying the polycarbonate resin.

REFERENCES

- 1 Hertzberg, R. W. and Manson, J. A. 'Fatigue of Engineering Plastics', Academic Press, New York, 1980
- 2 Budinski, K. G. 'Engineering Materials', Prentice-Hall, Englewood Cliffs, NJ, 1989
- 3 Sauer, J. A. and Hara, M. *Adv. Polym. Sci.* 1990, **91/92**, 67
- 4 Kusenko, V. S. and Tamusz, V. P. 'Fracture Micromechanics of Polymer Materials', Martinus, Boston, 1981
- 5 Takemori, M. T. *Adv. Polym. Sci.* 1983, **52/53**, 105
- 6 Doll, W. in 'Fractography and Failure Mechanisms of Polymers and Composites' (Ed. A. C. Roulin-Moloney), Elsevier, London, 1989, p. 387
- 7 Takemori, M. T. *Adv. Polym. Sci.* 1990, **91/92**, 263
- 8 Doll, W. and Konzol, L. *Adv. Polym. Sci.* 1990, **91/92**, 137
- 9 Mandell, J. F. and Chevaillier, J.-P. *Polym. Eng. Sci.* 1985, **25**, 170
- 10 Brown, H. R., Kramer, E. J. and Bubeck, R. A. *J. Polym. Sci., Polym. Phys. Edn.* 1987, **30**, 231
- 11 Takahara, A., Yamada, K., Kajiyama, T. and Takayanagi, M. *J. Appl. Polym. Sci.* 1980, **25**, 597
- 12 Takahara, A., Yamada, K., Kajiyama, T. and Takayanagi, M. *J. Appl. Polym. Sci.* 1981, **26**, 1085
- 13 Struik, L. C. *Polymer* 1980, **21**, 962
- 14 Smith, T. L., Ricco, T., Levita, G. and Moongan, W. K. *Plast. Rubber Proc.* 1985, **6**, 81
- 15 Bauwens-Crowet, C. and Bauwens, J. C. *Polymer* 1987, **28**, 1863
- 16 Wendorff, J. H. *Prog. Colloid Polym. Sci.* 1979, **66**, 135
- 17 Hristov, H. A., Yee, A. F., Xie, L. and Gidley, D. W. *Polymer* 1994, **35**, 4287
- 18 Hristov, H. A., Yee, A. F. and Gidley, D. W. *Polymer* 1994, **35**, 3604
- 19 Hashemi, S. and Williams, J. G. *Polym. Eng. Sci.* 1986, **26**, 760
- 20 Hashemi, S. and Williams, J. G. *Plast. Rubber Proc. Appl.* 1986, **6**, 363
- 21 Struik, L. C. E. 'Physical Aging in Amorphous Polymers and Other Materials', Elsevier, London, 1978
- 22 Ramos, A., Hutchinson, J. and Kovacs, A. J. *J. Polym. Sci., Polym. Phys. Edn.* 1984, **22**, 1665
- 23 Ruddy, M. and Hutchinson, J. *Polym. Commun.* 1988, **29**, 132
- 24 Hristov, H. A., Yee, A. F. and Gidley, D. W. to be published
- 25 Bouda, V., Zivlar, V. and Staverman, A. J. *J. Polym. Sci., Polym. Phys. Edn.* 1976, **14**, 2313